Proceedings of the 17th World Congress
The International Federation of Automatic Control
Seoul, Korea, July 6-11, 2008

Anti-Lock Braking System Using Predictive Control and On-Line Tire/Road Characteristics Estimation

A. Jacquet*, Y. Chamaillard,**
M. Basset*, G. Gissinger***, D. Frank*, J.P. Garcia***

** Messier-Bugatti, Safran Group, ZA Louis Bréguet,*
BP 40, 78141 Vélizy Cedex,France.
*** PRISM / LME – Université d'Orléans,*
8 rue Léonard de Vinci, 45072 Orléans Cedex 2, France.
**** University of Haute Alsace / MIPS Laboratory, ENSISA Lumière,*
12 rue des Frères Lumière, 68093 Mulhouse Cedex, France.

Abstract: A model predictive controller for optimal braking of a road vehicle is proposed. Taking into account the additional information provided by a torque sensor located in the wheel, there is no need to use any longitudinal model of the vehicle. Instead, we detail a way to identify a tire/road characteristic. This on-line reconstruction is based on an estimation of the longitudinal wheel slip and an estimation of the adhesion torque. The design approach, focused on the angular dynamics of the wheel, allows the use of the controller in vehicles for which assumptions on the longitudinal dynamics are not possible. Therefore, this controller is very indicated for aircraft applications.

1. INTRODUCTION

Braking performance is a main issue for road vehicles. In case of emergency, vehicle safety relies on the braking system which must provide maximum friction force and maintain directional control. However, excessive brake level results in the wheels being locked and the loss of vehicle controllability (Gissinger *et al.*, 2003). This phenomenon is well known and is due to the nonlinearity between the tire/road friction force and the wheel slip. The first solutions to improve braking efficiency simply consisted in preventing the lock of the wheel by means of Anti-lock Braking Systems (ABS). The control strategy was fairly simple at the beginning: the braking effort was increased or reduced based on the analysis of the dynamical behavior of the wheel. Such algorithms were far from perfect because they produced noticeable vibrations. In addition, strong oscillations of the brake level were harmful to the friction force maximization. Consequently, many theories and design methods have been proposed for decades, focused on ABS improvement. Some comparative studies can be found in (Chamaillard *et al.*, 1994a).

The techniques studied nowadays include sliding mode control (Drakunov *et al.*, 1995; El Hadri *et al.*, 2001), fuzzy logic (Yonggon and Stanislaw, 2002), optimal control (Petersen *et al.*, 2001), and predictive strategy (Anwar and Ashrafi, 2002). Traditionally, the control variables are either the wheel angular deceleration or the wheel slip but Savaresi *et al.* (2005) has recently suggested a combination of the two. Nevertheless, the main difficulty for the design of a brake controller is that the set point producing the maximum friction force is unknown and subject to variations. In a way, this issue remains independently of the controller design. To cope with the lack of a priori knowledge about the tire/road friction, Alvarez *et al.* (2000) proposed the use of a friction model estimation to set up an observer based controller.

Theses studies are most of the time related to automobile applications. As a consequence, the longitudinal deceleration is considered to be directly and exclusively linked with the tire/road friction force. Furthermore, the brake level is often supposed to be equally distributed on the wheels. For other applications, as aircraft braking, these hypotheses are not appropriate because of the effect of the aerodynamical forces, especially during landing phases, and because of the use of differential braking between the left and the right of the aircraft. For this kind of vehicle, the need is to improve the control without using any longitudinal model. Considering only the measures of the angular wheel velocity and the longitudinal speed, there is little chance to make significant progress in this direction. However, recent developments in brake torque measurement for commercial aircraft give a new hope. Chamaillard *et al.* (1994b) already raised the interest of the additional information provided by a torque sensor located in the wheel. In this paper, we take advantage of a newly available sensor to set up and adapt a tire/road characteristic model. This model is only based on the angular dynamics of the wheel. Then, a predictive controller can advantageously be designed to control the brake torque. Its natural anticipative behavior is well suited for the braking process.

This paper is organized as follows. System dynamics and tire/road adhesion phenomenon are described in section 2. Details on the predictive controller design are given in section 3. Section 4 presents the estimation principle of the tire/road characteristic. Some simulation results are provided in section 5. Finally, section 6 gives a short conclusion.

2. SYSTEM DYNAMICS

In this paper, we only consider the longitudinal dynamics of the vehicle. The longitudinal wheel speed is noted V and is assumed to equal the longitudinal vehicle speed.

2.1 Rotational dynamics of the wheel

The forces and torques applied to one wheel of the vehicle during a braking phase are presented in figure 1.

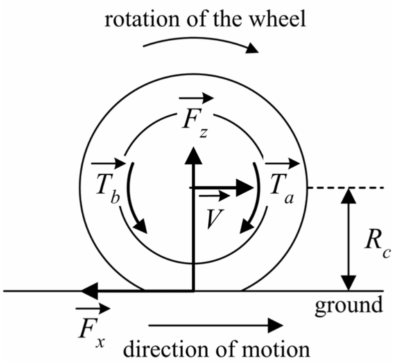

Fig. 1. Forces and torques applied during a braking phase

By neglecting the rolling resistance, generally insignificant compared to the torque produced by the friction force, the rotational dynamics of the wheel can simply be written:

$$J\,\dot{\omega} = T_b - T_a \tag{1}$$

where J is the moment of inertia of the wheel, ω is the angular velocity, T_b is the brake torque, T_a is the adhesion torque produced by the friction of the tire on the road surface. The relationship between the adhesion torque, the rolling radius of the wheel R_c and the friction force F_x is obvious:

$$T_a = R_c F_x \tag{2}$$

The friction force F_x is related to the vertical load F_z by the definition of a normalized friction coefficient μ:

$$F_x = \mu\, F_z \tag{3}$$

2.2 Adhesion coefficient behavior

Adhesion phenomenon is usually modeled with respect to the longitudinal wheel slip σ, computed from the longitudinal wheel speed V and the linear speed of the rolling tread $R_c\omega$:

$$\sigma = \frac{V - R_c\,\omega}{V} \tag{4}$$

Figure 2 gives some common shapes of the μ-σ curve for different kinds of road surface conditions.

The adhesion coefficient increases with the slip ratio until a limit σ_0 for which the adhesion equals its maximum value μ_0. After this limit, the adhesion coefficient begins to decrease.

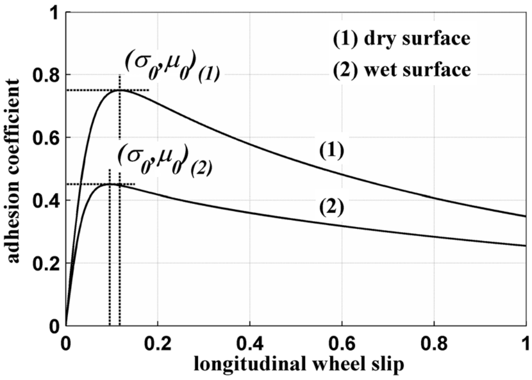

Fig. 2. Common shapes of μ-σ curves

The adhesion coefficient and the adhesion curve itself depend on several parameters: road surface, vehicle speed level, temperature, tire wear, etc. As a result, dynamic friction models are often preferred for control purposes (Alvarez *et al.*, 2000). But the main issue is that the set point σ_0 is never known accurately and subject to variations (figure 2). Moreover, the exact shape of the μ-σ curve cannot be known prior to braking. Its estimation must continuously be adapted to consider real case applications.

2.3 Maximization of the braking effect on the vehicle

Minimization of the braking distance is obtained by maximizing the friction force. Generally, this force is incorporated into the control law by considering the longitudinal vehicle dynamics (Drakunov *et al.*, 1995; Alvarez *et al.*, 2000; El Hadri *et al.*, 2001; Petersen *et al.*, 2001; Anwar and Ashrafi, 2002; Savaresi *et al.*, 2005):

$$M\,\frac{dV}{dt} = \sum_{k=1}^{n} F_{x,i} - F_a \tag{5}$$

where M is the mass of the vehicle, F_a the aerodynamic drag forces, $F_{x,i}$ the friction force on the i th wheel of the vehicle, which is supposed to comprise a total of n wheels.

If we do not want to make any assumption on F_a, the friction force F_x can hardly be used. Instead, the solution is to focus on T_a, remembering (2).

R_c varies according to the vertical load F_z, but in less proportion compared to the variation of μ (figure 2). So, maximizing the adhesion torque T_a gives a good mean to maximize the braking effect on the vehicle.

2.4 Estimation of the adhesion torque

The adhesion torque T_a can be estimated thanks to (1). First, we define ε_ω as an estimation error on the angular velocity:

$$\varepsilon_\omega = \omega_m - \hat{\omega} \tag{6}$$

where ω_m is the measure of the angular speed and $\hat{\omega}$ its estimation.

Using the angular accelerations $\dot{\omega}$ and $\hat{\dot{\omega}}$, (6) becomes:

$$\varepsilon_\omega = \omega_{m0} + \int_{t_0}^{t_0+T_e} \dot{\omega}\, dt - \hat{\omega}_0 - \int_{t_0}^{t_0+T_e} \hat{\dot{\omega}}\, dt \tag{7}$$

where ω_{m0} and $\hat{\omega}_0$ are the initial values of the integral terms at instant t_0, and T_e is the sample period.

Assume that the dynamical model (1) is true, we obtain:

$$\dot{\omega} = J^{-1}\left(T_b - T_a\right) \tag{8}$$

$$\hat{\dot{\omega}} = J^{-1}\left(T_{b,m} - \hat{T}_a\right) \tag{9}$$

where T_b and T_a represent real values, while $T_{b,m}$ and $\hat{T}_a$ are the measured brake torque and the estimated adhesion torque.

We can assume that the measure of the torque is not far from the real value: $T_{b,m} \approx T_b$. Then, if T_e is sufficiently small and after incorporating (8) and (9) in (7), ε_ω can be simplified as:

$$\varepsilon_\omega = \omega_{m0} - \hat{\omega}_0 + T_e\, J^{-1}\left(\hat{T}_a - T_a\right) \tag{10}$$

If we impose $\hat{\omega}_0 = \omega_{m0}$ at each sample time, (10) shows that the estimated torque converges to the real value when ε_ω tends to 0. This is obtained by introducing a retroaction loop between ε_ω and $\hat{T}_a$. For instance, with a simple retroaction loop, the estimation principle is outlined by figure 3.

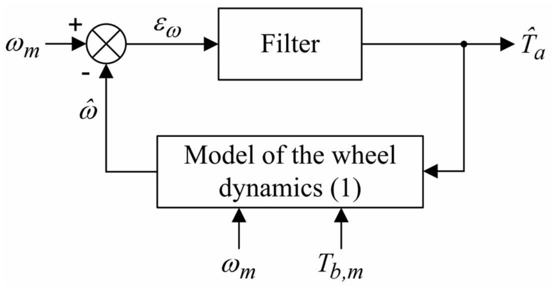

Fig. 3. Estimation of the adhesion torque

Simulation results (figure 4) show a good estimation even in the case of a signal with an additional perturbation (white noise). The tracking of the real value is fast and accurate.

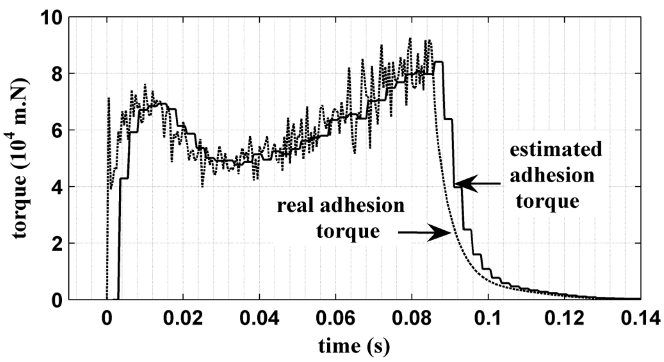

Fig. 4. Simulation results of the adhesion torque estimation

3. PREDICTIVE CONTROLLER DESIGN

The adhesion curve is a key element to the dynamical behavior of the wheel. Thus, a significant progress in braking strategies could be achieved by setting up a controller based on a model representative of the friction potential of the road. This model must be adapted on-line due to uncertainties about the tire/road characteristics and to take care of surface variations or puddles. In the case where the adhesion coefficient is unknown or difficult to estimate, we suggest a model describing the evolution of the adhesion torque with respect to the wheel slip.

In heavy applications, like commercial aircrafts, brake response time is small compared with wheel lock. For instance, a hydraulic brake can hardly respond faster than 90 ms while the wheel could lock in less than 150 ms. As a consequence, a predictive controller is advantageous because the strategy can anticipate the wheel skid. The time delay between the effective skid of the wheel and the decrease of the braking order can be reduced to its minimum. More general information on model predictive control can be found in (Clarke *et al.*, 1987a, b; Camacho *et al.*, 2004).

3.1 Control criterion

The control criterion defines the regulation objectives of the controller. If the control variable is the brake torque and the prediction horizon equals N, we can use the difference between angular reference speeds and the predicted ones:

$$C = \sum_{k=1}^{N}\left(\omega_{ref}(k) - \omega_{pred}(k)\right)^2 + \alpha \sum_{k=1}^{N} \Delta T_{b,c}(k)^2 \tag{11}$$

where ω_{ref} are the reference input speeds, ω_{pred} are the predicted speeds, α is a weighting coefficient, $T_{b,c}$ is the control variable of the brake and $\Delta T_{b,c}$ is the difference between two consecutive control variables in the future.

For the sake of simplicity, it is common to assume that the control variable $T_{b,c}$ remains constant during the whole prediction. Moreover, $T_{b,c}$ cannot exceed the maximum value $T_{b,max}$ allowed by the brake. In this case, the braking order is deduced by solving the minimization problem defined as:

$$min\ C\left(T_{b,c}\right) \text{ with } T_{b,c} \in [0; T_{b,max}] \tag{12}$$

Reference speeds are computed according to a given deceleration order $\dot{\omega}_c$ and the knowledge of the optimal slip σ_0. This value σ_0 can be deduced from a T_a-σ characteristic estimated on-line (section 4). First, we define:

$$\omega_{opt} = \left(1 - \sigma_0\right) R_c^{-1}\, V \tag{13}$$

Then, the reference speeds are computed in an iterative way:

$$\omega_{ref}(0) = \omega_m$$

$$k \in [1; N], \begin{cases} \omega_{ref}(k) = \omega_{ref}(k-1) + T_e\, \dot{\omega}_c \\ \omega_{ref}(k) = max\left(\omega_{ref}(k), \omega_{opt}\right) \end{cases} \tag{14}$$

To solve the problem (12), we need now to express ω_{pred} with respect to $T_{b,c}$.

3.2 Wheel speed prediction

According to (1) and considering the finite difference approximation of $\dot{\omega}$, a prediction of the wheel speed can be:

$$\omega_{pred}(1) = \omega_m + T_e\, J^{-1}\left(T_{b,m} - \hat{T}_a\right) \tag{15}$$

If we denote the T_a-σ characteristic as:

$$T_a = f(\sigma) \tag{16}$$

the one step prediction can be used iteratively:

$$\omega_{pred}(k+1) = \omega_{pred}(k) + T_e\, J^{-1}\left(T_{b,c} - f(\sigma(k))\right) \tag{17}$$

with

$$\sigma(k) = \left(V - R_c\, \omega_{pred}(k)\right)/V \tag{18}$$

Finally, writing $T_{b,c}$ in (17) is not accurate because it does not take into account the dynamic response of the brake. This can be done by considering a second order model, possibly integrating a time delay τ:

$$\frac{T_b}{T_{b,c}} = z^{-\tau}\, \frac{a_0 + a_1 z}{b_0 + b_1 z + b_2 z^2} \tag{19}$$

In its recursive form, (19) is rewritten:

$$\begin{aligned} T_b(k) = {} & \frac{a_0}{b_2} T_{b,c}(k-2-\tau) + \frac{a_1}{b_2} T_{b,c}(k-1-\tau) \\ & - \frac{b_0}{b_2} T_b(k-2) - \frac{b_1}{b_2} T_b(k-1) \end{aligned} \tag{20}$$

By regrouping (15), (16), (17), (18), (20) and defining the initial values as:

$$\begin{cases} \omega_{pred}(0) = \omega_m \\ T_b(0) = T_{b,m} \\ T_b(-1) = T_{b,m}(-1) \\ T_b(-2) = T_{b,m}(-2) \end{cases} \tag{21}$$

ω_{pred} is expressed with respect to $T_{b,c}$ with the following iterative system:

$$\begin{cases} \sigma(k) = \left(V - R_c\, \omega_{pred}(k)\right)/V \\ \hat{T}_a(k) = f(\sigma(k)) \\ T_b(k) = \dfrac{a_0}{b_2} T_{b,c}(k-2-\tau) + \dfrac{a_1}{b_2} T_{b,c}(k-1-\tau) \\ \qquad - \dfrac{b_0}{b_2} T_b(k-2) - \dfrac{b_1}{b_2} T_b(k-1) \\ \omega_{pred}(k+1) = \omega_{pred}(k) + T_e\, J^{-1}\left(T_b(k) - \hat{T}_a(k)\right) \end{cases} \tag{22}$$

where

$$\begin{cases} T_{b,c}(k) = T_{b,c}(k), & k-1-\tau \le 0 \\ T_{b,c}(k) = T_{b,c}, & k-1-\tau > 0 \end{cases} \tag{23}$$

Finally, (22) is repeated N times so that the wheel speeds are computed for the whole prediction horizon. The control variable $T_{b,c}$ can then be deduced from the minimization problem (12).

3.3 Minimization of the control criterion

Usually, a non linear minimization problem as (12) can easily be solved by linearizing the equations around the current set point. In our case, the fast dynamics of the system prevents to do so. Near the optimal set point σ_0, the linearization leads to a misinterpretation of the curve (figure 5).

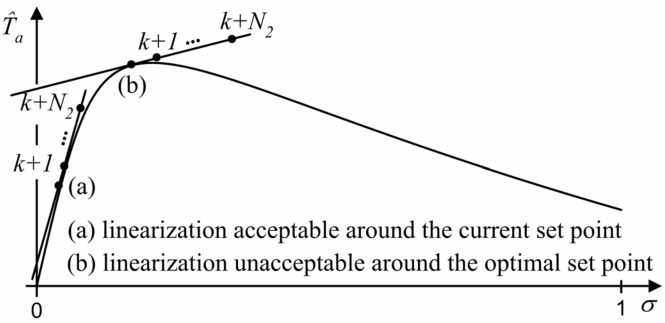

Fig. 5. Linearization issue near the optimal set point

Consequently, the problem (12) must be solved in a general non linear framework. For instance, the Levenberg-Marquardt method gives a very fast algorithm for non-linear least squares problems (Bonnans *et al.*, 2003).

The proof of the convexity of the control criterion, which ensures that the function has a unique global minimum, is not easy to obtain mathematically. Instead, we can study the dynamical behavior of the wheel and the shape of the control criterion for different values of the braking order.

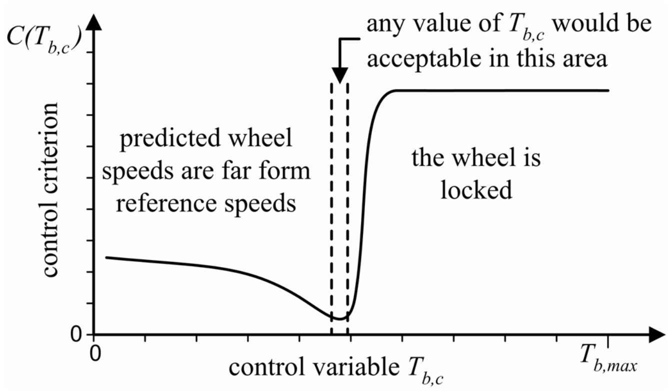

Fig. 6. Basic shape of the control criterion

For small values of $T_{b,c}$, the prediction model (22) yields to small values of wheel slip. As $T_{b,c}$ increases, the predicted wheel speeds reach the reference speeds. Then, for a certain value of $T_{b,c}$, the optimal set point is crossed. As a result, the wheel begins to lock and the predicted speeds move far from the reference speeds. The shape of the control criterion is thus characterized by 3 areas: middle, small and high (figure 6).

The exact determination of the minimum of $C(T_{b,c})$ is not required for a control point of view. A minimum found in the small values of the curve is sufficient to give a good control variable (figure 6). In a way, this approach can be considered as a sub-optimal control and greatly simplifies the implementation of the controller in case of real time constraint. Naturally, with such an analysis, the proof of the stability of the controller relies on a substantial number of simulation scenarios.

Finally, figure 7 gives an overview of our predictive controller and a representation of the flow of each variable.

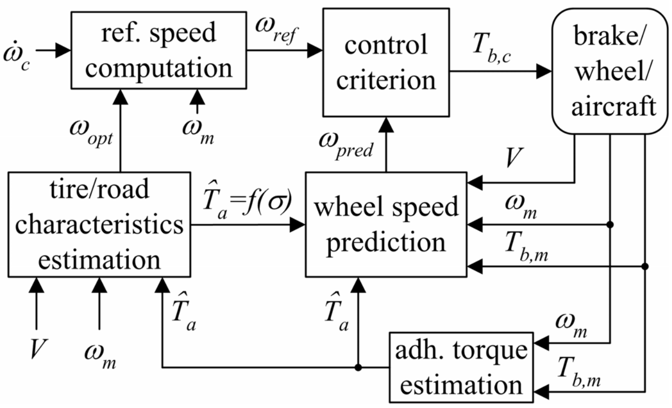

Fig. 7. Overview of the predictive controller

4. TIRE/ROAD CHARACTERISTICS ESTIMATION

The computation of the predictive model (22) is based on a good estimation of the T_a-σ characteristic (16).

4.1 Curve reconstruction principle

At each sample time, we have an estimation of the wheel slip with (4) and an estimation of the adhesion torque (figure 3). These two values define a single point in the T_a-σ plane. Then, by storing these data periodically since the beginning of the braking process, we obtain a data set from which the mathematical function (16) can be deduced (figure 8). Moreover, some a priori information taken from common tire characteristics are useful for the reconstruction of the curve. For instance, the first part of the curve corresponds to the vertical stiffness of the tire and is considered linear (figure 8). Furthermore, the optimal slip σ_0 is known to be greater than 5 % and smaller than 20 %. These bounds give some valuable constraints for the adaptation of the curve.

A good management of the incoming data allows a continuous adaptation in case of changes in the road surface condition (see figure 10). Finally, when the T_a-σ plane is empty, which occurs when no brake torque has been applied yet, a default T_a-σ function is used. Then the braking process starts and the plane is filled progressively.

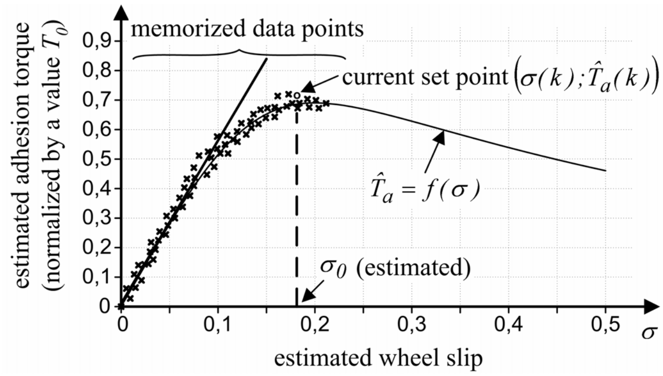

Fig. 8. Mathematical regression on the data set

4.2 Practical aspect of the regression

Due to the non linear shape of the T_a-σ model, a non linear regression is required. This regression consists in minimizing the square distance between the data points and the mathematical function. Therefore, considering some additional non linear constraints applied to this minimization, we fall into a general non linear minimization problem:

$$min \ \ \zeta(x) \quad s.t. \ \begin{cases} c_e(x) = 0 \\ c_i(x) \le 0 \\ x \in \Omega \end{cases} \tag{24}$$

where x is the vector of parameters defining the T_a-σ function, Ω its validity domain, ζ the square distance, c_e and c_i are respectively some equality and inequality constraints.

The minimization of such a problem can be achieved by the use a Quasi-Newton SQP algorithm. More information on numerical optimization can be found in (Bonnans *et al.*, 2003; Schittkowski and Zillober, 2004) and a practical implementation of a robust SQP algorithm is given in (Liu and Yuan, 2000).

For a real time implementation, the computational burden can be decreased by identifying some key elements of the curve, for instance: the slope of the linear part, the optimal slip, the maximum adhesion torque. Associated with a simple mathematical function, these elements give a numerical solution to the adaptation of the curve on the data set, which is also much faster than a classic regression process.

5. SIMULATION RESULTS

The predictive controller has been tested on dry and wet surfaces using the aircraft model of an Airbus A340-600 landed on runway. The prediction horizon was set to 200 ms, which allows a reliable prediction of the wheel lock with respect to the braking order. Each bloc of the control scheme shown figure 7 was sampled at 5 ms. This was obtained by distributing the control algorithms among two PowerPC running at 500 MHz. Figure 9 and 10 give simulation results for a change of road conditions between $t = 5$ s and $t = 9$ s.

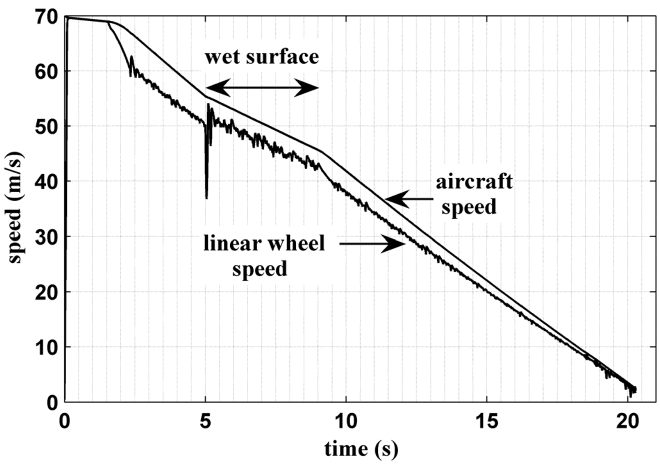

Fig. 9. Aircraft longitudinal speed and linear wheel speed

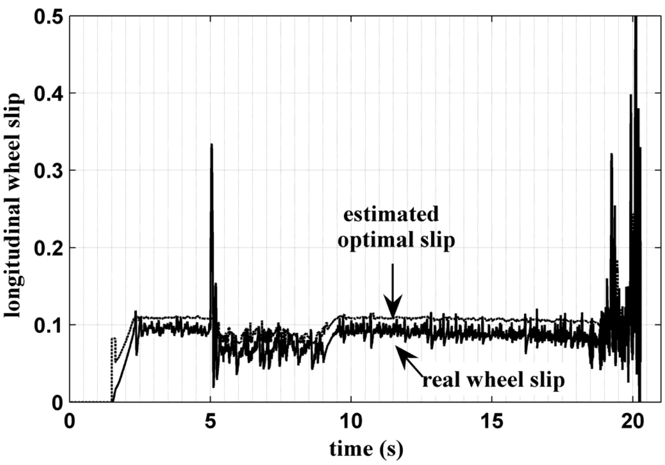

Fig. 10. Real wheel slip and estimated optimal set point

Our predictive controller gives good simulation results. The wheel skid is limited during the braking process even for small values of the speed, below 5 m/s (18 km/h). The optimal set point follows the changes in the road condition. It is higher on the dry surface than on the wet surface, which complies with real experiments. Finally, the braking distance obtained in figure 9 is 793 m. If the adhesion coefficient had remained perfectly at its maximum value, this distance would have been 751 m. In this case, we compute that the braking efficiency of our controller is about 94 % (751/793).

6. CONCLUSIONS

In spite of a higher computation load compared with other control methods, a drastic optimization of the algorithms allows a real time execution. The controller provides a fast adaptation to the change in surface condition and its stability is proven thanks to a sufficient number of simulation scenarios.

REFERENCES

Alvarez, A., J. Yi, R. Horowitz and C. Canudas de Wit (2000). Adaptive emergency braking control using a dynamic tire/road friction model. *IEEE Conference on Decision and Control*, **1**, pp. 456-461.

Anwar, S. and B. Ashrafi (2002). A predictive control algorithm for an anti-lock braking system. *SAE 2002 World Congress*, paper 2002-01-0302, Michigan, U.S.A.

Bonnans, J., J. Gilbert, C. Lemaréchal and C. Sagastizábal (2003). *Numerical Optimization*. Springer-Verlag, Heidelberg.

Camacho, E.F. and C. Bordons (2004). *Model Predictive Control.* Springer-Verlag, London.

Chamaillard, Y., G.L. Gissinger and C. Menard (1994a). Braking regulation of a vehicle, Application and comparison of control algorithms of unstable or pseudo-stable fast systems. *SAE Transaction*, paper 940837, U.S.A.

Chamaillard, Y., G.L. Gissinger, J.M. Perronne and M. Renner (1994b). An original braking controller with torque sensor. *IEEE Conference on Control Applications*, **1**, pp. 619-625.

Clarke, D.W., C. Mohtadi and P.S. Tuffs (1987a). Generalized Predictive Control - Part I. The basic algorithm. *Automatica*, **23**, pp. 137-148.

Clarke, D.W., C. Mohtadi and P.S. Tuffs (1987b). Generalized Predictive Control - Part II. Extensions and interpretations. *Automatica*, **23**, pp. 149-160.

Drakunov, S., Ü. Özgüner, P. Dix and B. Ashrafi (1995). ABS Control using optimum search via sliding mode. *IEEE Transactions on Control Systems Technology*, **3**, pp. 79-85.

El Hadri, A., J.C. Cadiou, K.N. M'Sirdi and Y. Delanne (2001). Wheel-slip regulation based on sliding mode approach. *SAE 2001 World Congress*, paper 2001-01-0602, Detroit, U.S.A.

Gissinger, G.L., C. Menard and A. Constans (2003). A mechatronic conception of a new intelligent braking system. *Control Engineering Practice*, **11**, pp. 163-170.

Liu, X.W. and Y.X. Yuan (2000). A robust algorithm for optimization with general equality and inequality constraints. *SIAM Journal on Scientific Computing*, **22**, pp. 517-534.

Petersen, I., T.A. Johansen, J. Kalkkuhl and J. Lüdemann (2001). Wheel slip control in ABS brakes using gain scheduled constrained LQR. *Proc. 6th European Control Conference*, pp. 606-611.

Savaresi, S. M., M. Tanelli, C. Cantoni, D. Charalambakis, F. Previdi and S. Bittanti (2005). Slip-deceleration control in anti-lock braking systems. *Proc. 16th IFAC World Congress*, paper Tu-A07-TO/6, pp. 1-6.

Schittkowski, K. and Ch. Zillober (2004). Nonlinear Programming: algorithms, software, and applications. In: *System Modeling and Optimization, Proc. 21th IFIP TC7 Conference*, (J. Cagnol, J.-P. Zolesio (Eds.)), **166**, pp. 73-108. Springer, U.S.A.

Yonggon, L. and H.Z. Stanislaw (2002). Designing a genetic neural fuzzy antilock-brake-system controller. *IEEE Transactions on Evolutionary Computation*, **6**, pp. 198-211.